

Syntheses, Vibrational Spectroscopy, and Crystal Structure Determination from X-Ray Powder Diffraction Data of Alkaline Earth Dicyanamides $M[\text{N}(\text{CN})_2]_2$ with $M = \text{Mg}, \text{Ca}, \text{Sr},$ and Ba

Barbara Jürgens, Elisabeth Irran, and Wolfgang Schnick¹*Department of Chemistry, University of Munich (LMU), Butenandtstrasse 5-13 (block D), D-81377 Munich, Germany*

Received July 17, 2000; in revised form November 1, 2000; accepted December 1, 2000; published online February 19, 2001

The alkaline earth dicyanamides $\text{Mg}[\text{N}(\text{CN})_2]_2$, $\text{Ca}[\text{N}(\text{CN})_2]_2$, $\text{Sr}[\text{N}(\text{CN})_2]_2$, and $\text{Ba}[\text{N}(\text{CN})_2]_2$ were synthesized by ion exchange using $\text{Na}[\text{N}(\text{CN})_2]$ and the respective nitrates or bromides as starting materials. The crystal structures were determined from X-ray powder diffractometry: $\text{Mg}[\text{N}(\text{CN})_2]_2$, $Pnmm$, $Z = 2$, $a = 617.14(3)$, $b = 716.97(3)$, and $c = 740.35(5)$ pm; $\text{Ca}[\text{N}(\text{CN})_2]_2$ and $\text{Sr}[\text{N}(\text{CN})_2]_2$, $C2/c$, $Z = 4$; $\text{Ca}[\text{N}(\text{CN})_2]_2$, $a = 1244.55(3)$, $b = 607.97(1)$, and $c = 789.81(1)$ pm, $\beta = 98.864(2)^\circ$; $\text{Sr}[\text{N}(\text{CN})_2]_2$, $a = 1279.63(2)$, $b = 624.756(8)$, and $c = 817.56(1)$ pm, $\beta = 99.787(1)^\circ$; $\text{Ba}[\text{N}(\text{CN})_2]_2$, $Pnma$, $Z = 4$, $a = 1368.68(7)$, $b = 429.07(7)$, and $c = 1226.26(2)$ pm. The dicyanamides consist of the respective alkaline earth cations and bent planar $[\text{N}(\text{CN})_2]^-$ ions. The structural features were correlated with vibrational spectroscopic data. The thermal behavior was studied by thermoanalytical experiments.

© 2001 Academic Press

Key Words: dicyanamides; alkaline earth metals; X-ray powder diffractometry; vibrational spectroscopy.

1. INTRODUCTION

In the past few years interest in transition metal dicyanamides $M^{\text{II}}[\text{N}(\text{CN})_2]_2$ and coordination compounds with $[\text{N}(\text{CN})_2]^-$ ligands has increased significantly because of their potential use as molecular magnets and organic superconductors, respectively (1, 2). Detailed information about the synthesis, characterization, and magnetic properties of $M[\text{N}(\text{CN})_2]_2$ ($M = \text{Cr}, \text{Mn}, \text{Co}, \text{Ni}, \text{Cu}, \text{Zn}$) has been given (2–6). Furthermore, several dicyanamides containing solvent molecules were characterized, e. g., $[\text{Cu}[\text{N}(\text{CN})_2]_2(\text{pyz})]_n$ (7) or $[\text{Fe}[\text{N}(\text{CN})_2]_2(\text{MeOH})_2]$ (8). Structural data for the dicyanamides with monovalent cations $\text{Ag}[\text{N}(\text{CN})_2]$ (9, 10), $\text{Li}[\text{N}(\text{CN})_2](\text{MeCN})_2$ (11), $\text{Cs}[\text{N}(\text{CN})_2]$ (12), and $\text{NaCs}_2[\text{N}(\text{CN})_2]_3$ (13) were communicated. The recently reported crystal structure of $\text{Na}[\text{N}(\text{CN})_2]$ (14) was of special

interest with regard to the trimerization of the $[\text{N}(\text{CN})_2]^-$ ions above 340°C leading to $\text{Na}_3\text{C}_6\text{N}_9$ which contains the cyclic tricyanomelaminato ion $[\text{C}_6\text{N}_9]^{3-}$.

The existence of alkaline earth dicyanamides has been assumed (15); however, no reliable information about their syntheses, crystal structures, or thermal behavior was available.

We now report on the syntheses and characterization of the alkaline earth dicyanamides $M[\text{N}(\text{CN})_2]_2$ ($M = \text{Mg}, \text{Ca}, \text{Sr}, \text{Ba}$) by X-ray powder diffractometry and vibrational spectroscopy. Thermoanalytical measurements were performed to investigate the possible formation of alkaline earth tricyanomelaminates $M_3(\text{C}_6\text{N}_9)_2$.

2. EXPERIMENTAL

2.1. Syntheses

The compounds $\text{Mg}[\text{N}(\text{CN})_2]_2$, $\text{Ca}[\text{N}(\text{CN})_2]_2$, $\text{Sr}[\text{N}(\text{CN})_2]_2$, and $\text{Ba}[\text{N}(\text{CN})_2]_2$ were prepared by ion exchange at room temperature. A column with an ion exchange resin (Merck, Ionenaustauscher I, Art. 4765) was completely filled with a solution of the respective alkaline earth salt [$\text{Mg}(\text{NO}_3)_2 \cdot 6\text{H}_2\text{O}$ (Fluka, p.a., >98%), $\text{Ca}(\text{NO}_3)_2 \cdot 4\text{H}_2\text{O}$ (Merck, p.a.), $\text{SrBr}_2 \cdot 6\text{H}_2\text{O}$ (95%, Alfa Aesar), $\text{BaBr}_2 \cdot 2\text{H}_2\text{O}$ (Riedel-de Haën, >98%)]. Any excess of these salts was removed by washing with water and subsequently a solution of $\text{Na}[\text{N}(\text{CN})_2]$ (Fluka, >96%) was poured onto the column. The eluate was collected and vacuum-dried. Under these conditions the alkaline earth dicyanamides were obtained as white microcrystalline powders.

2.2. X-Ray Structure Determination

For X-ray diffraction investigations powders of the compounds were enclosed in glass capillaries with 0.3 mm diameter. The measurements were carried out in Debye-Scherrer geometry on a STOE Stadi P powder diffractometer

¹To whom correspondence should be addressed. Fax: + 49/89 2180-7440. E-mail: wsc@cup.uni-muenchen.de.

TABLE 1
Crystallographic Data of the Alkaline Earth Dicyanamides

Formula	Mg[N(CN) ₂] ₂	Ca[N(CN) ₂] ₂	Sr[N(CN) ₂] ₂	Ba[N(CN) ₂] ₂
Formula weight	156.40	172.17	219.71	269.43
Crystal system	Orthorhombic	Monoclinic	Monoclinic	Orthorhombic
Space group	<i>Pnmm</i> (No. 58)	<i>C2/c</i> (No. 15)	<i>C2/c</i> (No. 15)	<i>Pnma</i> (No. 62)
Radiation (λ (pm))	CuKα ₁ (154.06)	CuKα ₁ (154.06)	CuKα ₁ (154.06)	MoKα ₁ (70.93)
Lattice constants (pm, °)	<i>a</i> = 617.14(3) <i>b</i> = 716.97(3) <i>c</i> = 740.35(5)	<i>a</i> = 1244.55(3) <i>b</i> = 607.97(1) <i>c</i> = 789.81(1) β = 98.864(2)	<i>a</i> = 1279.63(2) <i>b</i> = 624.756(8) <i>c</i> = 817.56(1) β = 99.787(1)	<i>a</i> = 1368.68(7) <i>b</i> = 429.07(7) <i>c</i> = 1226.26(2)
Volume (10 ⁶ pm ³)	327.58(3)	590.48(2)	644.10(2)	720.14(1)
<i>Z</i>	2	4	4	4
ρ _c (g/cm ³)	1.585	1.936	2.265	2.485
Profile range	5° ≤ 2θ ≤ 80°	3° ≤ 2θ ≤ 80°	3° ≤ 2θ ≤ 80°	3° ≤ 2θ ≤ 50°
No. of data points	7500	7700	7700	4700
No. of reflections	110	183	194	725
Positional params	12	22	22	25
Profile params	17	16	19	16
<i>R</i> values	wR _p = 0.109 R _p = 0.086 R _F = 0.071	wR _p = 0.097 R _p = 0.077 R _F = 0.045	wR _p = 0.073 R _p = 0.057 R _F = 0.020	wR _p = 0.066 R _p = 0.053 R _F = 0.038

with Ge(111)-monochromatized radiation (CuKα₁ for Mg[N(CN)₂]₂, Ca[N(CN)₂]₂, Sr[N(CN)₂]₂; MoKα₁ for Ba[N(CN)₂]₂) using a PSD. The Rietveld refinements were performed with the program GSAS (16). In order to describe the profile of the X-ray reflections a pseudo-Voigt function (17) with a special asymmetry (18) was used. Details of the crystallographic data are listed in Table 1; the refined atomic coordinates of the compounds are given in Tables 2–4.

The diffraction pattern of Mg[N(CN)₂]₂ could be indexed with similar lattice constants and the same space group as the transition metal dicyanamides M[N(CN)₂]₂ (*M* = Cr, Mn, Co, Ni, Cu) (2–5) which turned out to be isotypic. The atomic coordinates of Ni[N(CN)₂]₂ (3) were used as starting values for the Rietveld refinement of Mg[N(CN)₂]₂ (Fig. 1). The dicyanamides Ca[N(CN)₂]₂ and Sr[N(CN)₂]₂ crystallize in the space group *C2/c* (No. 15) and the two compounds are isostructural. The crystal

structure of Sr[N(CN)₂]₂ was solved by *ab initio* crystal structure determination from X-ray powder diffraction data using the programs EXTRA (19) for extraction of the integrated intensities and SIRPOW (20) for direct methods. The atomic coordinates determined for Sr[N(CN)₂]₂ were also used as starting values for the Rietveld refinement of Ca[N(CN)₂]₂ (Figs. 2 and 3). Ba[N(CN)₂]₂ crystallizes in the orthorhombic space group *Pnma* (No. 62). Its crystal structure was determined by *ab initio* structure determination with EXTRA and SIRPOW, as well. The results of the refinement are given in Fig. 4. The diffraction patterns of

TABLE 3
Atomic Coordinates and Displacement Factors (pm²) of Ca[N(CN)₂]₂ (Above) and Sr[N(CN)₂]₂ (Below)

Atom	Wyckoff position	<i>x</i>	<i>y</i>	<i>z</i>	<i>U</i> _{iso} ^a
Ca	4e	0	0.0982(3)	$\frac{1}{4}$	429(7)
Sr	4e	0	0.0965(1)	$\frac{1}{4}$	334(3)
C1	8f	0.2263(5)	0.4709(9)	0.3050(8)	475(23)
	8f	0.2280(4)	0.4676(8)	0.3146(6)	349(20)
C2	8f	0.0845(4)	0.6216(10)	0.4085(7)	349(22)
	8f	0.0878(4)	0.6152(9)	0.4099(6)	357(19)
N1	8f	0.3126(4)	0.4779(7)	0.2698(6)	428(20)
	8f	0.3082(4)	0.4691(6)	0.2754(6)	464(19)
N2	8f	0.1259(3)	0.4472(9)	0.3424(5)	398(23)
	8f	0.1295(3)	0.4456(7)	0.3460(4)	285(16)
N3	8f	0.0384(3)	0.7650(7)	0.4627(5)	396(20)
	8f	0.0436(3)	0.7543(6)	0.4598(4)	265(16)

^a *U*_{iso} is defined as exp (− 8π²*U*_{iso} sin² θ/λ²).

^a *U*_{iso} is defined as exp (− 8π²*U*_{iso} sin² θ/λ²).

TABLE 2
Atomic Coordinates and Displacement Factors (pm²) of Mg[N(CN)₂]₂

Atom	Wyckoff position	<i>x</i>	<i>y</i>	<i>z</i>	<i>U</i> _{iso} ^a
Mg	2a	0	0	0	572(15)
C	8h	− 0.2647(9)	0.1531(8)	0.3448(9)	558(29)
N1	8h	− 0.2057(7)	0.0974(6)	0.2112(4)	478(23)
N2	4g	− 0.3334(9)	0.2257(7)	$\frac{1}{2}$	427(28)

TABLE 4
Atomic Coordinates and Displacement Factors (pm^2)
of $\text{Ba}[\text{N}(\text{CN})_2]_2$

Atom	Wyckoff position	x	y	z	U_{iso}^a
Ba	4c	0.2124(2)	$\frac{1}{4}$	0.3771(2)	212(3)
C1	4c	0.012(2)	$\frac{1}{4}$	0.614(4)	160(40)
C2	4c	0.175(2)	$\frac{1}{4}$	0.671(2)	160(40)
C3	4c	0.167(2)	$\frac{1}{4}$	0.066(2)	160(40)
C4	4c	0.007(2)	$\frac{1}{4}$	0.152(3)	160(40)
N1	4c	-0.074(2)	$\frac{1}{4}$	0.612(3)	317(26)
N2	4c	0.113(2)	$\frac{1}{4}$	0.591(2)	317(26)
N3	4c	0.235(2)	$\frac{1}{4}$	0.746(2)	317(26)
N4	4c	0.213(2)	$\frac{1}{4}$	0.009(2)	317(26)
N5	4c	0.103(2)	$\frac{1}{4}$	0.161(2)	317(26)
N6	4c	-0.075(2)	$\frac{1}{4}$	0.151(3)	317(26)

^a U_{iso} is defined as $\exp(-8\pi^2 U_{\text{iso}} \sin^2 \theta / \lambda^2)$; the displacement factors of C and N, respectively, are constrained to be equal.

$\text{Mg}[\text{N}(\text{CN})_2]_2$, $\text{Ca}[\text{N}(\text{CN})_2]_2$, and $\text{Sr}[\text{N}(\text{CN})_2]_2$ revealed a remaining small portion of the starting material $\text{Na}[\text{N}(\text{CN})_2]$.

2.3. Vibrational Spectroscopic Investigations

Infrared spectra were recorded on a Bruker IFS 66v/S spectrometer scanning a range from 400 to 4000 cm^{-1} . The samples were thoroughly mixed with dried KBr (5 mg sample, 500 mg KBr). Raman spectra were excited by a Bruker FRA 106/S module with an Nd-YAG laser ($\lambda = 1064 \text{ nm}$) scanning a range from 100 to 3500 cm^{-1} . All preparation procedures have been performed in a glovebox under a dried argon atmosphere.

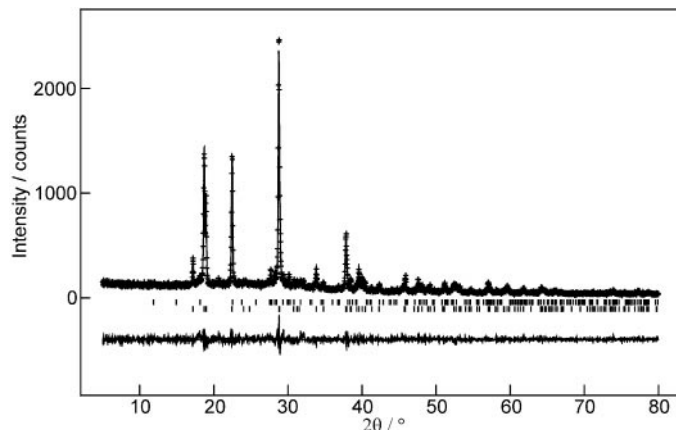


FIG. 1. Observed (crosses) and calculated (line) X-ray powder diffraction pattern as well as a difference profile of the Rietveld refinement of $\text{Mg}[\text{N}(\text{CN})_2]_2$. The lower row of vertical lines indicates possible peak positions of $\text{Mg}[\text{N}(\text{CN})_2]_2$, the upper row those of $\text{Na}[\text{N}(\text{CN})_2]$.

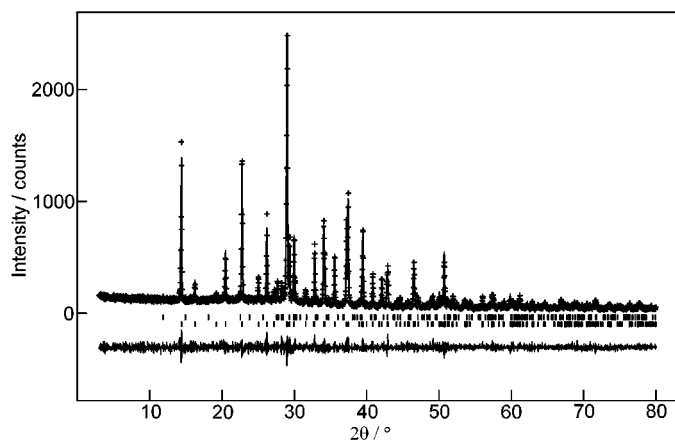


FIG. 2. Observed (crosses) and calculated (line) X-ray powder diffraction pattern as well as a difference profile of the Rietveld refinement of $\text{Ca}[\text{N}(\text{CN})_2]_2$. The lower row of vertical lines indicates possible peak positions of $\text{Ca}[\text{N}(\text{CN})_2]_2$, the upper row those of $\text{Na}[\text{N}(\text{CN})_2]$.

2.4. Thermal Behavior Investigations

Differential scanning calorimetry (DSC) curves of the salts $\text{M}[\text{N}(\text{CN})_2]_2$ were recorded under a dried N_2 atmosphere with a Mettler DSC 25 from room temperature to 500°C (heating rate 10°C/min).

Samples of the salts were heated in sealed glass ampoules under an argon atmosphere to different temperatures between 200°C and 500°C. After cooling beige-brown powders were obtained, which were characterized by powder diffraction.

Temperature-dependent X-ray measurements were performed on a STOE Stadi P powder diffractometer ($\text{MoK}\alpha_1$ radiation) with a computer-controlled STOE furnace. The

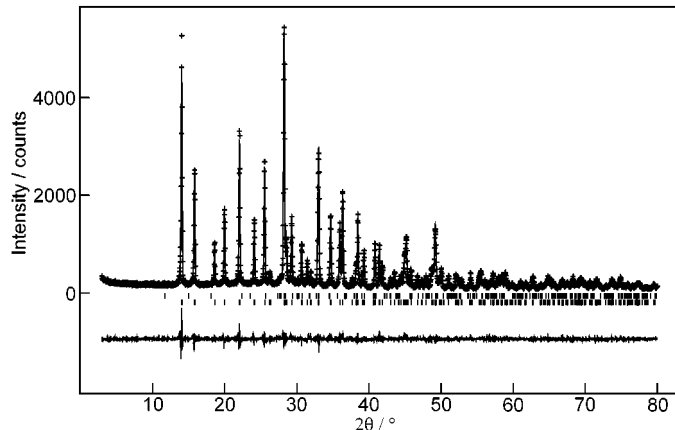


FIG. 3. Observed (crosses) and calculated (line) X-ray powder diffraction pattern as well as a difference profile of the Rietveld refinement of $\text{Sr}[\text{N}(\text{CN})_2]_2$. The lower row of vertical lines indicates possible peak positions of $\text{Sr}[\text{N}(\text{CN})_2]_2$, the upper row of those $\text{Na}[\text{N}(\text{CN})_2]$.

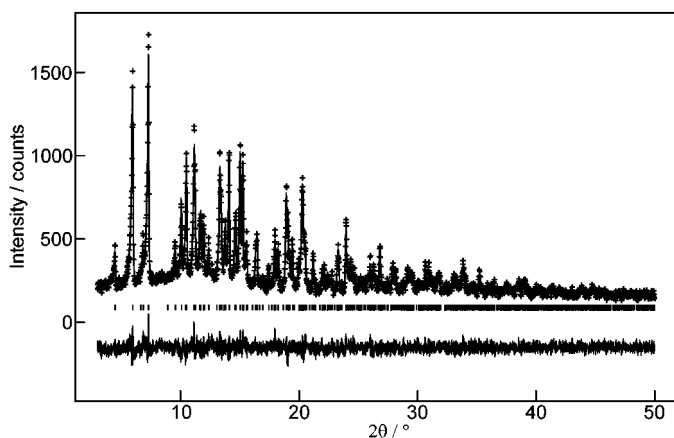


FIG. 4. Observed (crosses) and calculated (line) X-ray powder diffraction pattern as well as a difference profile of the Rietveld refinement of $\text{Ba}[\text{N}(\text{CN})_2]_2$. The vertical lines indicate the possible peak positions of $\text{Ba}[\text{N}(\text{CN})_2]_2$.

samples were enclosed in quartz capillaries and heated from room temperature to 500°C in steps of 20°C .

3. RESULTS

3.1. The Crystal Structure of $\text{Mg}[\text{N}(\text{CN})_2]_2$

Magnesium dicyanamide $\text{Mg}[\text{N}(\text{CN})_2]_2$ crystallizes isostructurally with the transition metal dicyanamides $M[\text{N}(\text{CN})_2]_2$ ($M = \text{Cr}^{2+}$, Mn^{2+} , Co^{2+} , Ni^{2+} , Cu^{2+}) (2–5). The crystal structures of these compounds derive from the rutile type (Fig. 5). The cations are octahedrally coordinated by six N atoms and the $[\text{N}(\text{CN})_2]^-$ groups are bound to three cations. The ionic radius of Mg^{2+} (72 pm) is comparable to the bivalent transition metal ions mentioned above (Cr^{2+} , 80; Mn^{2+} , 83; Co^{2+} , 75; Ni^{2+} , 69; and Cu^{2+} , 73 pm) (21). Accordingly their salts frequently are isotypic.

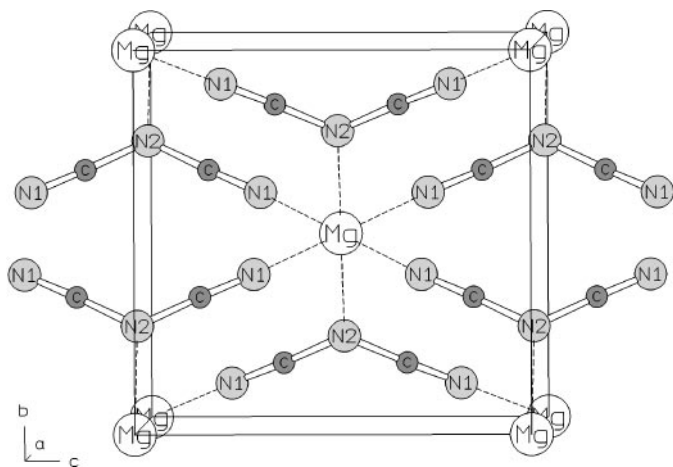


FIG. 5. Crystal structure of $\text{Mg}[\text{N}(\text{CN})_2]_2$, view along $[100]$.

TABLE 5
Bond Distances (pm) and Angles ($^\circ$) in $\text{Mg}[\text{N}(\text{CN})_2]_2$

Mg–N1	213.1(4) ($4\times$)
Mg–N2	221.9(5) ($2\times$)
C–N1	112.8(7)
C–N2	133.0(6)
N1–C–N2	177.7(7)
C–N2–C	119.4(8)

The $[\text{N}(\text{CN})_2]^-$ ions of $\text{Mg}[\text{N}(\text{CN})_2]_2$ are bent and planar (point symmetry C_s); the distances and angles are comparable to those of other dicyanamides (Table 5). The distances N–CN from the central N atoms are longer (133 pm) than those to the terminal N atoms (112 pm), representing single and triple bonds, respectively. The N1–C–N2 angles are almost linear (177°), whereas the C–N2–C angle is 119° .

3.2. The Crystal Structures of $\text{Ca}[\text{N}(\text{CN})_2]_2$ and $\text{Sr}[\text{N}(\text{CN})_2]_2$

The dicyanamides $\text{Ca}[\text{N}(\text{CN})_2]_2$ and $\text{Sr}[\text{N}(\text{CN})_2]_2$ are isotypic. The structures consist of M^{2+} ions arranged in layers which are connected by the $[\text{N}(\text{CN})_2]^-$ ions (Figs. 6 and 7). The cations are surrounded by eight N atoms of eight different $[\text{N}(\text{CN})_2]^-$ ions which form an irregular quadratic antiprism. Two of them (N2) are bridging atoms of the $[\text{N}(\text{CN})_2]^-$ ions, and the others six are terminal ones (N1, N3). In the crystal the $[\text{N}(\text{CN})_2]^-$ ions have site symmetry C_1 , but analogously to $\text{Mg}[\text{N}(\text{CN})_2]_2$ the anions are bent and planar exhibiting nearly C_{2v} symmetry.

The distances and angles (Table 6) show the usual values for dicyanamides (bridging C–N bonds, 132–133 pm; terminal C–N bonds, 112–116 pm; N–C–N, 172 – 175° ; C–N–C, 115 – 116°).

The crystal structures of $\text{Ca}[\text{N}(\text{CN})_2]_2$ and $\text{Sr}[\text{N}(\text{CN})_2]_2$ resemble that of $\text{Pb}(\text{SCN})_2$ (22) where the coordination sphere of Pb^{2+} and the arrangement of the anions are comparable. A replacement of the S atom of the thiocyanate ion by an NCN group nearly transforms the structure of $\text{Pb}(\text{SCN})_2$ into that of $\text{Ca}[\text{N}(\text{CN})_2]_2$.

3.3. The Crystal Structure of $\text{Ba}[\text{N}(\text{CN})_2]_2$

In barium dicyanamide $\text{Ba}[\text{N}(\text{CN})_2]_2$ all atoms are situated on layers parallel to (010) at $y = \frac{1}{4}$ and $\frac{3}{4}$, respectively (Fig. 8). Ba^{2+} is coordinated by three N's of the layers above and below, respectively, which form a trigonal prism. With an additional three N's of the same layer the coordination sphere of Ba^{2+} is formed by a three-capped prism of nine N's (Fig. 9). Two of the N's, which cap the prism faces, are bridging N's (N2, N5), and all others are terminal.

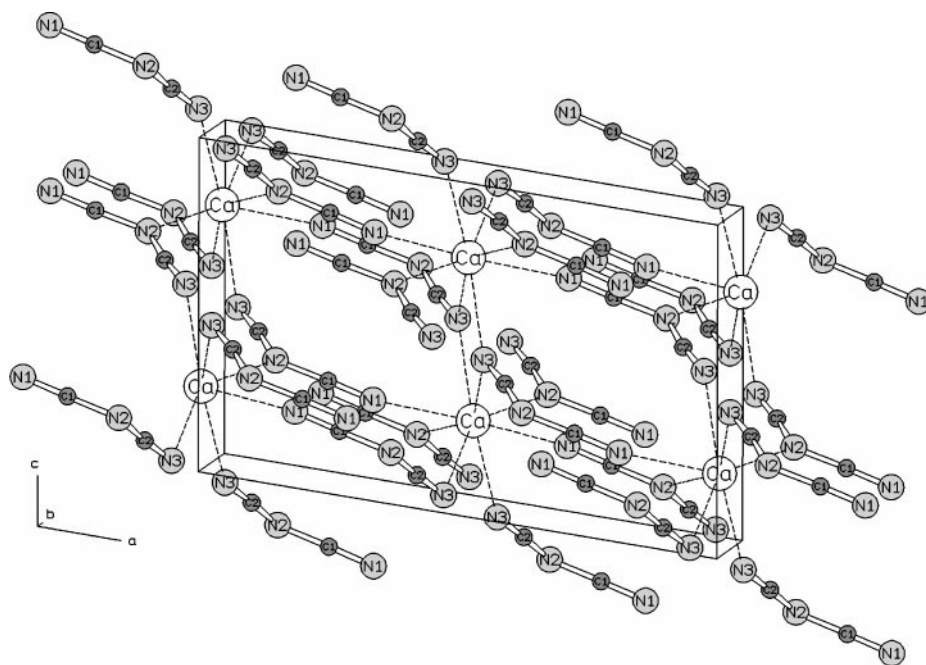


FIG. 6. Crystal structure of $\text{Ca}[\text{N}(\text{CN})_2]_2$, view along $[010]$; the crystal structure of $\text{Sr}[\text{N}(\text{CN})_2]_2$ is analogous.

In $\text{Ba}[\text{N}(\text{CN})_2]_2$ there are two crystallographically different $[\text{N}(\text{CN})_2]^-$ ions, and the respective N atoms of both ions are differently coordinated to Ba^{2+} . In the first anion (N4–C3–N5–C4–N6) only one terminal N (N4) is bound to two cations, comparable to the situation in $\text{Ca}[\text{N}(\text{CN})_2]_2$ or $\text{Sr}[\text{N}(\text{CN})_2]_2$. In the other anion both terminal N's (N1, N3) are neighboring two cations. The existence of two differently coordinated $[\text{N}(\text{CN})_2]^-$ ions is also seen in the IR spectrum

of $\text{Ba}[\text{N}(\text{CN})_2]_2$, where specific vibrations show a significant splitting (Fig. 10). Both anions have the crystallographic site symmetry C_s , but they nearly approach C_{2v} . The interatomic distances (Table 7) are comparable to those of other dicyanamides, but they could not be determined as accurately as in the other dicyanamides due to the more complicated structure and the lower resolution of the diffraction pattern.

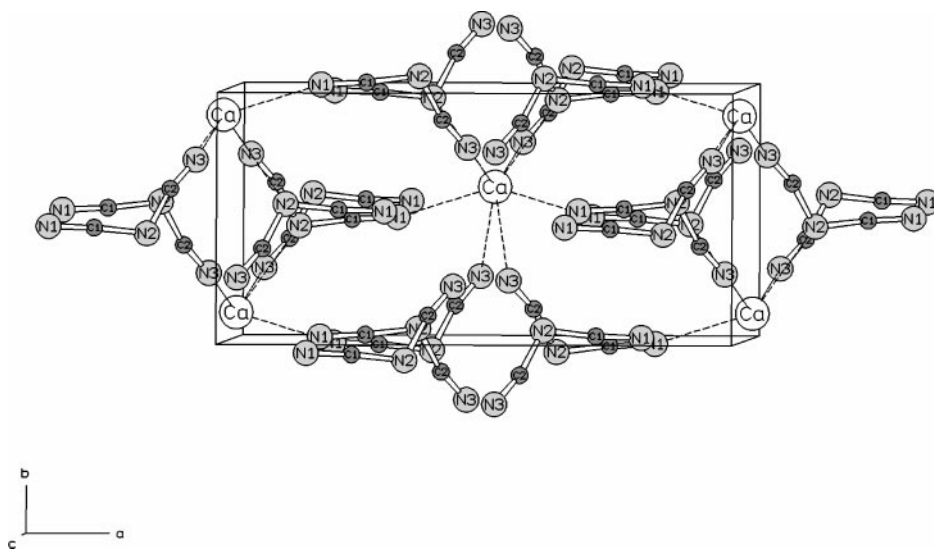


FIG. 7. Crystal structure of $\text{Ca}[\text{N}(\text{CN})_2]_2$, view along $[001]$.

TABLE 6
Bond Distances (pm) and Angles ($^{\circ}$) in $\text{Ca}[\text{N}(\text{CN})_2]_2$
and $\text{Sr}[\text{N}(\text{CN})_2]_2$

	Ca	Sr
M-N1	247.2(5) (2 \times)	262.2(4) (2 \times)
M-N2	267.2(5) (2 \times)	277.1(4) (2 \times)
M-N3	262.8(4) (2 \times)	273.8(4) (2 \times)
M-N3	253.1(4) (2 \times)	269.5(4) (2 \times)
C1-N1	115.2(7)	112.6(5)
C1-N2	133.5(6)	133.5(5)
C2-N2	132.1(7)	133.3(5)
C2-N3	116.1(7)	114.9(5)
N1-C1-N2	175.8(7)	172.4(7)
N2-C2-N3	173.3(7)	174.2(6)
C1-N2-C2	115.8(6)	116.6(5)

TABLE 7
Bond Distances (pm) and Angles ($^{\circ}$) in $\text{Ba}[\text{N}(\text{CN})_2]_2$

Ba-N1	287(1) (2x)	Ba-N2	295(3)
Ba-N3	278(2) (2 \times)	Ba-N5	304(3)
Ba-N4	288(2) (2 \times)	Ba-N6	293(2)
C1-N1	117(3)	C3-N4	93(4)
C1-N2	142(3)	C3-N5	146(3)
C2-N2	129(3)	C4-N5	132(3)
C2-N3	123(3)	C4-N6	113(3)
N1-C1-N2	167(5)	N4-C3-N5	176(4)
N2-C2-N3	178(3)	N5-C4-N6	176(5)
C1-N2-C2	119(3)	C3-N5-C4	122(3)

As the crystal structure of $\text{Mg}[\text{N}(\text{CN})_2]_2$ can be derived from the AB_2 compound rutile, $\text{Ba}[\text{N}(\text{CN})_2]_2$ is related to the cotunnite-type (PbCl_2), another AB_2 -type. This structure type is adopted by a number of halides and chalcogenides where the cations have the highest coordination number for AB_2 ionic compounds.

[Further details of the crystal structure investigations may be obtained from the Fachinformationszentrum Karlsruhe, D-76344 Eggenstein-Leopoldshafen, Germany (fax (49) 7247-808-666; e-mail crysdata@fiz-karlsruhe.de) on quoting the depository numbers CSD-411361 ($\text{Mg}[\text{N}(\text{CN})_2]_2$), CSD-411362 ($\text{Ca}[\text{N}(\text{CN})_2]_2$), CSD-411363 ($\text{Sr}[\text{N}(\text{CN})_2]_2$), and CSD-411364 ($\text{Ba}[\text{N}(\text{CN})_2]_2$).]

3.4. Vibrational Spectroscopic Properties

The IR and Raman spectra (Figs. 10 and 11) of the alkaline earth dicyanamides show the typical band sequence of a five-atom molecular ion with point symmetry C_{2v} . The

observed frequencies are given in Table 8. The signals at 2150–2310 cm^{-1} show the existence of a triple bond between C and the terminal N atoms of the $[\text{N}(\text{CN})_2]^-$ ion. The remarkable signals at 1310–1330 cm^{-1} belong to the asymmetric stretching mode ($\nu_{\text{as}}\text{N-C}$) of the bridging N and the C atoms. Above 3000 cm^{-1} only small signals were observed which belong to combinational vibrations, accordingly the samples are free of any N-H bonds. A detailed interpretation of the modes of the $[\text{N}(\text{CN})_2]^-$ ion is given in (13).

Compared to the other alkaline earth metal dicyanamides $\text{Mg}[\text{N}(\text{CN})_2]_2$ shows the highest frequencies for most of the vibrations. The frequencies of $\text{Ca}[\text{N}(\text{CN})_2]_2$ and $\text{Sr}[\text{N}(\text{CN})_2]_2$ are nearly the same, differing only by about 10 cm^{-1} . In most cases the frequencies of $\text{Ca}[\text{N}(\text{CN})_2]_2$ are the higher of the two. No definite trend is seen for the split signals of $\text{Ba}[\text{N}(\text{CN})_2]_2$. The higher ones of them mainly show a bigger value than the respective signals of $\text{Ca}[\text{N}(\text{CN})_2]_2$ and $\text{Sr}[\text{N}(\text{CN})_2]_2$ and the lower ones have smaller frequencies compared to those of the signals for the other alkaline earth metal dicyanamides. The trend of decreasing frequencies from $\text{Mg}[\text{N}(\text{CN})_2]_2$ to $\text{Ba}[\text{N}(\text{CN})_2]_2$ could be explained by the decreasing bond strengths. The

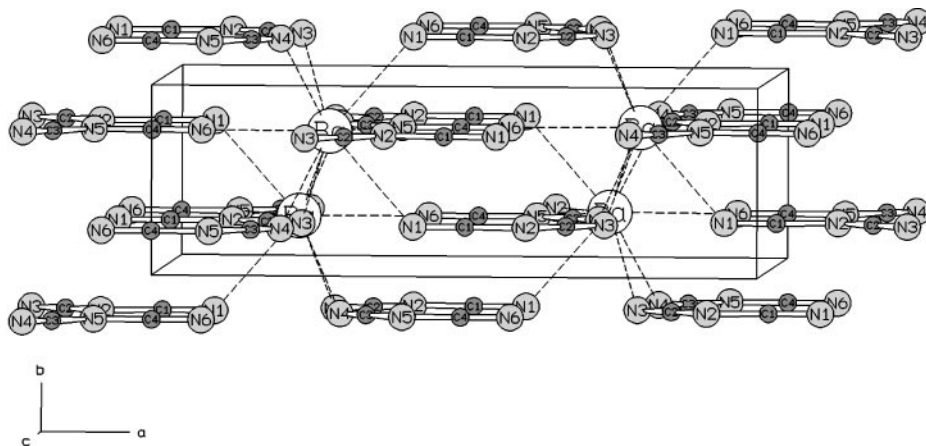


FIG. 8. Crystal structure of $\text{Ba}[\text{N}(\text{CN})_2]_2$, view along $[001]$.

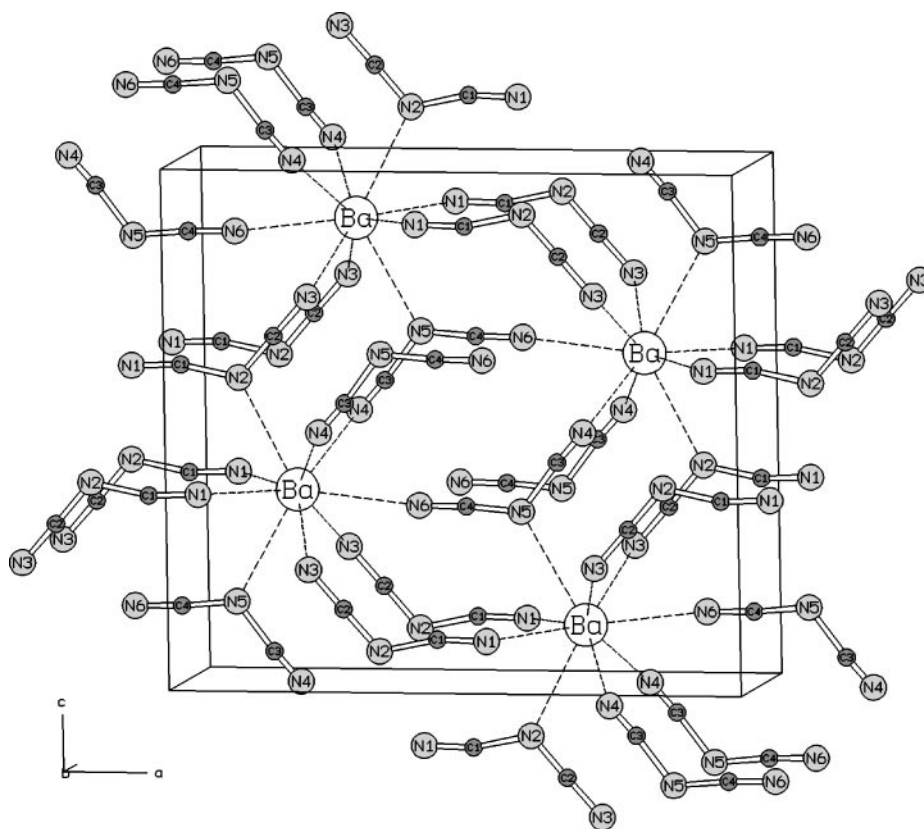


FIG. 9. Crystal structure of $\text{Ba}[\text{N}(\text{CN})_2]_2$, view along $[010]$.

bridging N atoms are connected to only one M^{2+} ion in all four compounds, but the connectivities of the terminal N atoms are different. In $\text{Mg}[\text{N}(\text{CN})_2]_2$ all of them are coordinated to one Mg^{2+} ion, in $\text{Ca}[\text{N}(\text{CN})_2]_2$ and $\text{Sr}[\text{N}(\text{CN})_2]_2$ half of the terminal N atoms are connected to two metal ions, and in $\text{Ba}[\text{N}(\text{CN})_2]_2$ three-fourths of them are connected to two Ba^{2+} ions. The more metal ions

coordinate the dicyanamide ion, the weaker are the bond strengths inside them and the smaller are the frequencies.

3.5. Thermal Behavior

During heating dicyanamide ions $[\text{N}(\text{CN})_2]^-$ are able to trimerize to tricyanomelaminato ions $[\text{C}_6\text{N}_9]^{3-}$ as was re-

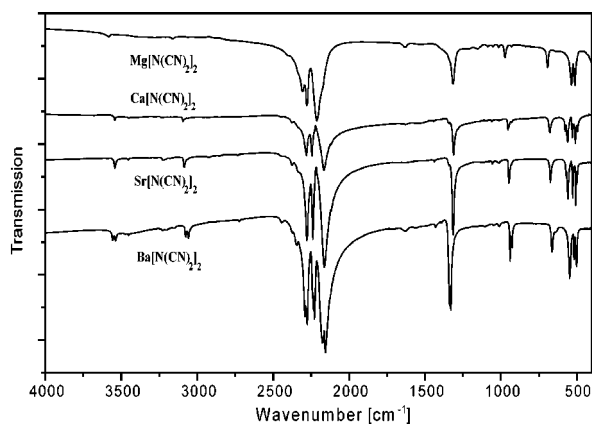


FIG. 10. Infrared spectra of the alkaline earth dicyanamides $M[\text{N}(\text{CN})_2]_2$.

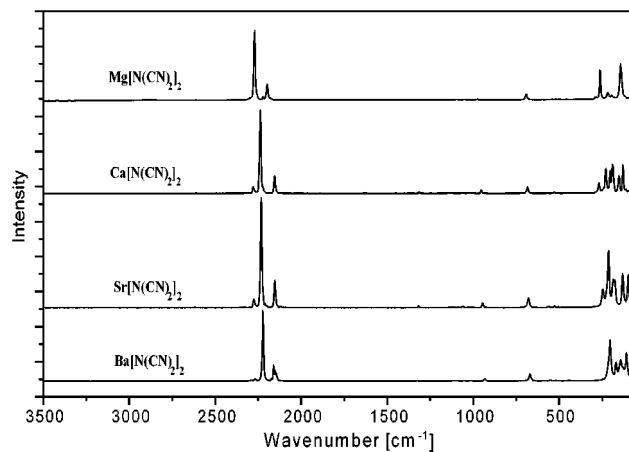


FIG. 11. Raman spectra of the alkaline earth dicyanamides $M[\text{N}(\text{CN})_2]_2$.

TABLE 8
Vibrational Frequencies of the Alkaline Earth Dicyanamides (cm⁻¹)^a

Mg[N(CN) ₂] ₂	Ca[N(CN) ₂] ₂	Sr[N(CN) ₂] ₂	Ba[N(CN) ₂] ₂	Vibration
3582.4(w)	3542.7(w)	3542.0(w)	3556.0/3538.2(w)	IR ν _s C≡N + ν _{as} N-C
	3451.2(w)	3454.0(w)	3474.3/3450.6(w)	IR ν _{as} C≡N + ν _{as} N-C
	3230.0(w)	3221.0(w)	3225.8/3202.1(w)	IR ν _s C≡N + ν _s N-C
3161.8(w)	3093.8(w)	3086.0(w)	3078.0/3058.2(w)	IR ν _{as} C≡N + ν _s N-C
2306.5(s)	2281.6(s)	2277.5(s)	2289.0/2276.4(s)	IR ν _s C≡N
2278.4(s)	2244.6(s)	2238.9(s)	2235.9/2228.3(s)	IR ν _{as} N-C + ν _s N-C
2271.6(vs)	2237.9(vs)	2232.6(vs)	2220.5(vs)	Ra ν _s C≡N
2222.1(m)	2278.7(w)	2275.0(w)	2292.2/2269.7(w)	Ra
2212.2(vs)	2164.4(vs)	2163.4(vs)	2174.3/2172.8(vs)	IR ν _{as} C≡N
2197.7(m)	2153.9(m)	2153.2(m)	2160.0/2150.0(m)	Ra ν _{as} C≡N
	1314.4(w)	1318.4(w)	1326.4(w)	Ra ν _{as} N-C
1316.0(s)	1311.9(s)	1314.7(s)	1340.3/1331.1(s)	IR ν _{as} N-C
972.8(m)	954.1(m)	947.4(m)	939.7/927.9(m)	IR ν _s N-C
	952.5(w)	945.8(w)	932.4(w)	Ra ν _s N-C
692.8(m)	678.3(m)	673.9(m)	663.8(m)	IR δ _s N-C≡N
690.8(w)	683.5(w)	678.2(w)	670.8(w)	Ra δ _s N-C≡N
535.0(m)	577.6(w)	558.9(m)	547.3/540.9(m)	IR deformation
	567.8(w)	526.3(w)	553.1(w)	Ra vibrations
	561.0(m)		518.3(m)	IR
	529.6(w)	527.3(w)	518.3/508.3(w)	Ra
	529.1(w)			IR
512.6(m)	510.1(m)	507.5(m)	508.2/501.2(m)	IR
	505.6(w)	504.9(w)		Ra
	495.6(w)			IR
			444.7/416.6(m)	Ra
< 300	< 300	< 300	< 300	Ra lattice vibrations

^a vs: very strong; s: strong; m: medium; w: weak.

cently demonstrated for Na[N(CN)₂]₂ (14). With regard to the possible formation of alkaline earth tricyanomelaminates M₃(C₆N₉)₂ (M = Mg, Ca, Sr, Ba) the thermal behavior of the salts M[N(CN)₂]₂ (M = Mg, Ca, Sr, Ba) is of special interest.

During temperature-dependent *in situ* investigations on the powder diffractometer the reflections of the dicyanamides M[N(CN)₂]₂ disappeared and the samples became X-ray amorphous (Mg, >440°C; Ca, >400°C; Sr, >280°C; Ba, >360°C). After cooling all samples remained X-ray amorphous. Thus, the phase transitions apparently are irreversible, and a further structural characterization of the formed products by X-ray investigations was not possible.

The DSC curves show broad exothermic peaks (Mg[N(CN)₂]₂, 440–500°C; Ca[N(CN)₂]₂, 350–450°C; Sr[N(CN)₂]₂, 320–350°C; Ba[N(CN)₂]₂, 320–340 and 350–440°C). The observed thermal effects indicate a transformation of the dicyanamide ions [N(CN)₂]⁻.

In the vibrational spectra of the heated samples broad signals were observed which belong to C≡N and C=N bonds, but do not belong to monomeric [N(CN)₂]⁻ ions. Probably there is an s-triazine ring (C₃N₃) but the spectrum is not typical of isolated [C₆N₉]³⁻ ions. Similar spectra

were recorded for the heated transition metal dicyanamides Co[N(CN)₂]₂ and Ni[N(CN)₂]₂ (B. Jürgens, M. Kurmoo, and W. Schnick, unpublished results). Presumably the alkaline earth dicyanamides as well as the transition metal dicyanamides transform not to tricyanomelaminates ions, but to salts with hitherto unknown oligomeric or polymeric C-N anions.

ACKNOWLEDGMENTS

Financial support by the Fonds der Chemischen Industrie, Germany, the Bundesministerium für Bildung und Forschung (project 03-SC5LMU-5), and especially the Deutsche Forschungsgemeinschaft (Gottfried-Wilhelm-Leibniz-Programm) is gratefully acknowledged.

REFERENCES

1. A. M. Kini, U. Geiser, H. H. Wang, K. D. Carlson, J. M. Williams, W. K. Kwok, K. G. Vandervoort, J. E. Thompson, D. L. Stupka, D. Jung, and M.-H. Whangbo, *Inorg. Chem.* **29**, 2555 (1990).
2. M. Kurmoo and C. J. Kepert, *J. New. Chem.* **2**, 1515 (1998).
3. J. L. Manson, C. R. Kmetz, Q.-Z. Huang, J. W. Lynn, G. M. Bendele, S. Pagola, P. W. Stephens, L. M. Liabe-Sands, A. L. Rheingold, A. J. Epstein, and J. S. Miller, *Chem. Mater.* **10**, 2552 (1998).

4. S. R. Batten, P. Jensen, B. Moubaraki, K. S. Murray, and R. Robson, *Chem. Commun.* 439 (1998).
5. J. L. Manson, D. W. Lee, A. L. Rheingold, and J. S. Miller, *Inorg. Chem.* **37**, 5966 (1998).
6. J. L. Manson, C. R. Kmety, A. J. Epstein, and J. S. Miller, *Inorg. Chem.* **38**, 2552 (1999).
7. P. Jensen, S. R. Batten, G. D. Fallon, D. C. R. Hockless, B. Moubaraki, K. S. Murray, and R. Robson, *J. Solid State Chem.* **145**, 387 (1999).
8. J. L. Manson, A. M. Arif, and J. S. Miller, *J. Mater. Chem.* **9**, 979 (1999).
9. D. Britton and Y. M. Chow, *Acta Crystallogr. Sect. B* **33**, 697 (1977).
10. D. Britton, *Acta Crystallogr. Sect. C* **46**, 2297 (1990).
11. A. P. Purdy, E. Houser, and C. F. George, *Polyhedron* **16**, 3671 (1997).
12. P. Starynowicz, *Acta Crystallogr. Sect. C* **47**, 2198 (1991).
13. B. Jürgens, W. Milius, P. Morys, and W. Schnick, *Z. Anorg. Allg. Chem.* **624**, 91 (1998).
14. B. Jürgens, E. Irran, J. Schneider, and W. Schnick, *Inorg. Chem.* **39**, 665 (2000).
15. E. C. Franklin, *J. Am. Chem. Soc.* **44**, 486 (1922).
16. A. C. Larson and R. B. von Dreele, General Structure Analysis System, Report LAUR 86-748, Los Alamos National Laboratory, Los Alamos, NM, 1990.
17. P. Thompson, D. E. Cox, and J. B. Hastings, *J. Appl. Crystallogr.* **20**, 79 (1987).
18. L. W. Finger, D. E. Cox, and A. P. Jephcoat, *J. Appl. Crystallogr.* **27**, 892 (1994).
19. A. Altomare, M. C. Burla, G. Cascarano, C. Giacovazzo, A. Guagliardi, A. G. G. Moltineri, and G. Polidori, *J. Appl. Crystallogr.* **28**, 842 (1995).
20. A. Altomare, G. Cascarano, C. Giacovazzo, A. Guagliardi, M. C. Burla, G. Polidori, and M. Camalli, *J. Appl. Crystallogr.* **27**, 435 (1994).
21. R. D. Shannon, *Acta Crystallogr. Sect. A* **32**, 751 (1976).
22. J. A. A. Mokuolu and J. C. Speakman, *Acta Crystallogr. Sect. B* **31**, 172 (1975).